Pakistan Veterinary Journal

ISSN: 0253-8318 (PRINT), 2074-7764 (ONLINE)
DOI: 10.29261/pakvetj/2023.119

RESEARCH ARTICLE

Chondrocyte Apoptosis as a Potential Mechanism in Ostrich Limb and Toe Disorders: A Pathological Investigation

Miao Xian[#], Bowen Duan[#], Li Tang[*], Hongxu Zhou, Le Wang, Ronghui Wang, Zhengli Chen, Jing Fang, Chao Huang, Wentao Liu, Yi Geng, Ping OuYang, Hongrui Guo, Huidan Deng and Weimin Lai

[1]Department of Basic Veterinary Medicine, College of Veterinary Medicine, Sichuan Agricultural University, Chengdu 611134, P.R. China
*Corresponding author: tangyimingtt@163.com

ARTICLE HISTORY (23-216)

Received: June 3, 2023
Revised: November 26, 2023
Accepted: November 29, 2023
Published online: December 28, 2023

Key words:
Ostrich leg and toe disease
Tarsal joint
Cartilage
Apoptosis
Bcl-2/Bax

ABSTRACT

Avian toe-legged disease poses serious threat to ostrich farms worldwide. Despite its severity, the underlying pathogenic mechanism of toe- legged disease in ostrich remains elusive. Our study aims to explore the connection between toe leg disease and articular cartilage with prime focus on the underlying mechanism in the pathogenesis of the disease. For this purpose, 18 male ostriches, comprising three groups: group A (6 healthy), group B (6 with mild disease), and group C (6 with severe disease), all aged 3 months were selected. Histopathological changes in tarsal joints of ostriches with leg and toe disease were observed using radiological examination (X-ray), Hematoxylin and Eosin (H&E), Safranin O-staining, and Masson trichome staining. The chondrocytes were evaluated for apoptosis and changes in the expression of Bcl-2 and Bax in articular cartilage using TdT-mediated dUTP Nick-End Labeling (TUNEL), and Immunohistochemistry (IHC). The results indicated that the tarsal joints of ostriches with leg and toe disease exhibit pathological changes such as thickening of the periosteum, decreased number of chondrocytes, shallow staining of cartilage matrix, incomplete tidemark, and decreased collagen. In comparison to Group A, there was a significant decrease in cell apoptosis ($P<0.01$) while the expression of apoptosis proteins Bcl-2 and Bax was found to be significantly increased ($P<0.01$) in the tarsal cartilage of groups B and C. In conclusion, our findings suggest that excessive chondrocyte apoptosis may be the underlying pathogenic mechanism for toe and leg disease in ostriches. These findings offer valuable insights for the diagnosis and treatment of ostriches with toe-legged disease.

To Cite This Article: Xian M, Duan BW, Tang L, Zhou HX, Wang L, Wang RH, Chen ZL, Fang J, Huang C, Liu WT, Geng Y, OuYang P, Guo HR, Deng HD and Lai WM, 2024. Chondrocyte apoptosis as a potential mechanism in ostrich limb and toe disorders: a pathological investigation. Pak Vet J, 44(1): 71-78. http://dx.doi.org/10.29261/pakvetj/2023.119

INTRODUCTION

The African ostrich holds significant economic value and is widely favored by the the majority of the farmers. Nevertheless, toe-legged diseases in ostrich farms are associated with substantial morbidity and mortality, presenting clinical manifestations including claudication, paralysis, depression, and, in severe cases, death. In prior findings, the differences between this particular lesion of toe legged disease and bone lesions in ostriches resulting from bacterial infection (Peel *et al.*, 2022), parvovirus infection (Yuan *et al.*, 2020), impaired calcium and phosphorus metabolism and absorption (Venäläinen *et al.*, 2006), or fractures (Wander *et al.*, 2000) were discerned completely highlighting a huge difference. In contrast to the aforementioned scenarios, toe and leg disease in ostriches typically manifests tarsal joint swelling. However, the pathomorphology and pathogenesis of ostrich leg and toe disease has remained unexplored so far.

Among clinical manifestations of joint swelling, osteoarthritis (OA) usually predominates which is often influenced by congenital and acquired factors (Wang, 2018). Conversely, bone anomalies in cats and dogs primarily result from fractures (Ma *et al.*, 2021), providing limited relevance to this study. Nevertheless, extensive research on human bone diseases, including OA and rheumatoid arthritis (RA) (Go *et al.*, 2022), has revealed that pathological changes in joint swelling predominantly involve damage to joint cartilage. Articular

cartilage plays a pivotal role in maintaining joint motion function. In normal joint activities, articular cartilage ensures efficient sliding and stress transmission between articular surfaces, and is extremely important in bearing, transmitting, and releasing pressure (Loeser *et al.,* 2012). Hence, our study focuses on ostrich tarsal cartilage.

In studies examining osteoarthritis (OA) in animal models, like rats there has been a focus on evaluating chondrocytes (Li, 2021). Similarly, in companion animals such as horses, dogs and cats OA is characterized by apoptosis. This suggests that apoptosis plays a role in the occurrence and development of OA (Yuan *et al.,* 2022). Apoptosis is a process responsible for removing senescent and mutated cells during the production of new cells. It promotes the functioning and metabolism of organs and tissues (Huang *et al.,* 2018). Any abnormalities in apoptosis can disrupt internal environment balance and function resulting in damage and impacting the onset, progression and prognosis of diseases. Therefore, our study aims to investigate apoptosis as part of understanding this disease.

Recent research findings (Ni *et al.,* 2021) have highlighted that Bcl 2 and Bax are indicators for detecting OA and RA. The B cell lymphoma 2 (Bcl 2) family genes are found widely throughout organisms. They consist of genes, like Bcl 2 and Bcl 2 associated X (Bax) which represent both promotive aspects of apoptosis. Bcl 2 plays a role, in controlling cell survival by preventing apoptosis while Bax greatly speeds up the death signal triggering cell apoptosis (Willis *et al.,* 2003). In a body there is an equilibrium, between Bcl 2 and Bax. However, when this balance is disturbed, it can result in cell apoptosis and various pathological alterations (Kourtis *et al.,* 2018).

In this study, we aim to investigate the histopathological changes in the cartilage of the tarsal joint in ostriches affected by toe-leg disease. Specifically, we seek to explore the potential association between abnormal chondrocyte apoptosis and the expression of Bcl-2 and Bax genes in the context of this disease. This exploration is believed to contribute valuable insights in the diagnosis and treatment of toe-legged disease affecting major population of ostriches.

MATERIALS AND METHODS

Experimental design: All experimental procedures were opted after ethical approval of ----with reference no SYXK 2019-187. African ostriches were selected for adaptive feeding in a uniform batch before the experiment. These ostriches were procured from the Sanmu ostrich breeding farm in Mianyang City, Sichuan Province. Briefly, a total of 18 male ostriches, aged 3 months, were included in the study. The animals were categorized into three groups: Group A (6 healthy ostriches), Group B (6 ostriches with mild disease), and Group C (6 ostriches with severe disease). Selection criteria for diseased ostriches included:

1. Depression and difficulty in feeding.
2. Swollen tarsal joints and lameness.
3. Inability to stand.
4. Exclusion of other joint diseases such as infection, bone tumor, and fracture.

Group B ostriches needed to meet criteria 1, 2 and 3 while Group C ostriches needed to meet criteria 1, 2, 3 and 4. Additionally, the classification was verified using Mankin's score as a reference (Mankin *et al.,* 1971; Cheng *et al.,* 2022) as described in Table 1.

Radiological assessments: The animals were sedated with Ketamine and Xylazine before radiography. The ostriches were placed laterally on the operating table with an X-ray window of the generator directed at the tarsal joint of the ostrich for transmission. The exposure parameters were set at 60kVp and 5.0 mAs.

Histomorphometric analysis: The tarsal joint circumference of each ostrich was measured with a tape measure immediately after slaughter. For histological studies, the articular cartilage from the tarsal joint was fixed in 4% paraformaldehyde for 48 hours. Subsequently, decalcification was performed using a 10% EDTA solution at a pH of approximately 7. The decalcified samples were embedded, and consecutive paraffin sections were obtained for staining with Hematoxylin and Eosin (H&E) Safranin O, and Masson Trichome as per manufacturer's guidelines. While, some sections were used for terminal - deoxynucleotidyl transferase-mediated nick end labeling (TUNEL) and immunohistochemistry (IHC).

TUNEL assay: For TUNEL Assay, TUNEL Apoptosis Detection Kit IV (CY3) (Bode Bioengineering Co., LTD) was used. Briefly, the cartilage paraffin sections are dewaxed and digested with 0.01 M TBS (Tris-buffered saline) containing freshly diluted protease K (1:200) at 37 °C for 15 min followed by 3 times washing with 0.01 M TBS. Subsequently, sections were labeled with a solution comprising terminal deoxynucleotidyl transferase (TdT) and DIG-d-UTP mixed proportionally with labeling buffer for 2 hours at 37°C, followed by three washes with 0.01 M TBS. Afterward, blocking solution was applied at room temperature for 30 minutes, and excess blocking solution was removed without washing. Biotinylated anti-digoxin antibodies are diluted 1:100 and incubated with the sections at 37°C reaction for 30 minutes followed by three washes with 0.01 M TBS. In the next step, SABC-FITC (streptavidin-biotin complex conjugated with fluorescein isothiocyanate) (SABC（Rabbit IgG）-POD Kit, Beijing Soleibao Biotechnology Co., LTD) was diluted 1:100 and applied at 37°C for 30 minutes, followed by four washes with 0.01 M TBS. Finally, sections were treated with an anti-fluorescent attenuating agent, and fluorescence microscopy was employed for observation. The presence of green fluorescent granules within the nucleus indicated positive cells, specifically apoptotic cells. TUNEL's sections were scanned using the Panoramic sections Scanner, then opened with Case Viewer 2.4 software and viewed under 10×40X lenses. The number of apoptotic cells and the total number of cells in the target area of each slice were quantified using the Indica Labs-High Plex FL v3.1.0 module in the Halo v3.0.311.314 analysis software to find the apoptosis rate (%).

Immunohistochemistry staining: For IHC, sections of articular cartilage were dewaxed in xylene, rehydrated through graded ethanol concentrations, then rinsed with distilled water, PBS and peroxidase solution respectively.

Table 1: The modified Mankin's scoring criteria for joint cartilage in ostriches with toe-legged disease.

Cartilage structure	Score	Chondrocytes	Score	Matrix staining	Score	Integrity of the tidal line	Score
Light as usual	0	The quantity is as usual	0	normal	0	complete	0
Surface destruction	1	Diffuse increase	1	Mild loss of staining	1	Multiple tidal lines	1
Destruction of blood vessels and superficial layers	2	A large number of cluster-like cell clumps appear	2	Moderate staining	2	Subchondral vascular invasion of tidal lines	2
Shallow fissures form up to the migratory layer	3	The number has decreased significantly	3	Severe loss of staining	3		
The fissure reaches as deep as the radiation layer	4			The staining disappears completely	4		
The fissure reaches deep into the calcified layer	5						
Complete destruction of the structure	6						

The sections were then, incubated overnight at 4°C with primary antibodies Rabbit Anti-Bcl-2 and Rabbit Anti-Bax antibodies (please mention dilution), and rinsed 3 times in PBS. Afterwards, the sections were incubated for 20 min at room temperature with secondary antibody (please mention name and dilution). SABC (streptavidin-biotin complex) was added dropwise to the sections at room temperature and allowed to react for 20 minutes. The bound antibodies were observed under microscope following incubation with DAB (3,3'-diaminobenzidine), and the sections were rinsed for 1-2 times with distilled water, Finally, sections were counterstained with hematoxylin, dehydrated, cleared, and mounted for microscopic examination. The positive results were judged by the presence of yellow or brownish-yellow particles.

The results of IHC were quantified by using the Image Pro Plus 6.0 image analysis system. For this purpose, 5 tissue sections per ostrich (n = 6 per group) were selected and observed at 10×40X magnification under microscopes (BX51; Olympus, Tokyo, Japan), For careful readings, each section intercepted 10 fields of view according to a unified standard to determine the integral light density (IOD) of the positive product.

Statistical analysis: SPSS 22.0 software was used for statistical analysis, and the obtained data were expressed as mean ± standard deviation (M±SD), and the significance of the difference was analyzed by t-test. $P<0.05$ was assumed as a significant difference, and $P<0.01$ as extremely significant difference.

RESULTS

Clinical observation showed that compared with healthy ostriches, ostriches with toe-leg disease were lethargic, with rough hair, unable to stand, and with swollen tarsal joints (Fig. 1A). The tarsal joint circumference of ostriches with toe-legged disease was greater than that of healthy ostriches and increased with the increase of disease (Fig. 1D). The X-ray results showed that the joint capsule of the tarsal joint of the ostrich with leg disease was enlarged, the synovial fluid increased, small osteophytes appeared in the cartilage concave, and the subchondral bone was sclerotic (Fig. 1B); The result of joint section showed that the cartilage of the tarsal joint was rough and soft, with a dull color, of which a few cartilages in group C were accompanied by defects (Fig. 1C).

Histological analysis

H&E staining: The H&E results indicated that compared with group A, the groups B and C, (Fig. 2A, D), revealed notable pathological alterations. The surface perichondrium exhibited thickening with associated changes including necrosis in middle cartilage cells and cellular reduction. Additionally, the deep tide line within the convex and concave regions of the cartilage appeared incomplete. Furthermore, compared with group B, subchondral vascular invasion tide line, inflammatory cell infiltration, and more chondrocyte necrosis were more prominent in the deep layer of group C.

Masson trichome staining: The Masson trichrome staining indicated that within groups B and C, an evident decline was observed in the cartilage matrix and collagen fibers, accompanied by pronounced fibrosis. Notably, there was a significant reduction in bone collagen within the cartilage convex and cartilage concave of ostrich tarsal joints (Fig. 2B, E).

Safranin O-fast green staining: As a result of Safranin O staining, it was observed that in groups B and C, the matrix component decreased, the proteoglycan safranin staining was lighter in the cartilage matrix, and the content of glycosaminoglycans was found to be reduced, in the cartilage convex and cartilage concave of ostrich tarsal joint (Fig. 2C, F).

Based on the above results, we found that the scores of diseased ostriches were significantly higher than those of healthy ostriches ($P<0.01$), and the score of group C was extremely significant ($P<0.01$), greater than group B (Fig. 1E), From this, we can conclude that it is consistent with Mankin's scoring criteria.

TUNEL analysis: TUNEL results showed that the apoptotic cells were green, and located in the middle layer of cartilage (Fig. 3A, B). The chondrocyte apoptosis rate of tarsal cartilage convex and cartilage concave in groups B and C was significantly higher than that in group A ($P<0.01$), and the chondrocyte apoptosis rate in group C was significantly higher than that in group B ($P<0.01$) (Fig. 3C, D).

IHC analysis: IHC results showed that the Bcl-2 and Bax proteins located in the cartilage matrix and cellular nucleus of chondrocytes in articular cartilage of the tarsal joints (Fig. 4). In groups B and C, the expression levels of Bcl-2 and Bax proteins in the cartilage convex and cartilage concave were significantly higher ($P<0.01$) than those in group A; the expression levels of Bcl-2 and Bax proteins in group C were extremely significant ($P<0.01$) compared to group B. Compared with group A, the Bcl-2/Bax ratio of articular cartilage of the tarsal joints in

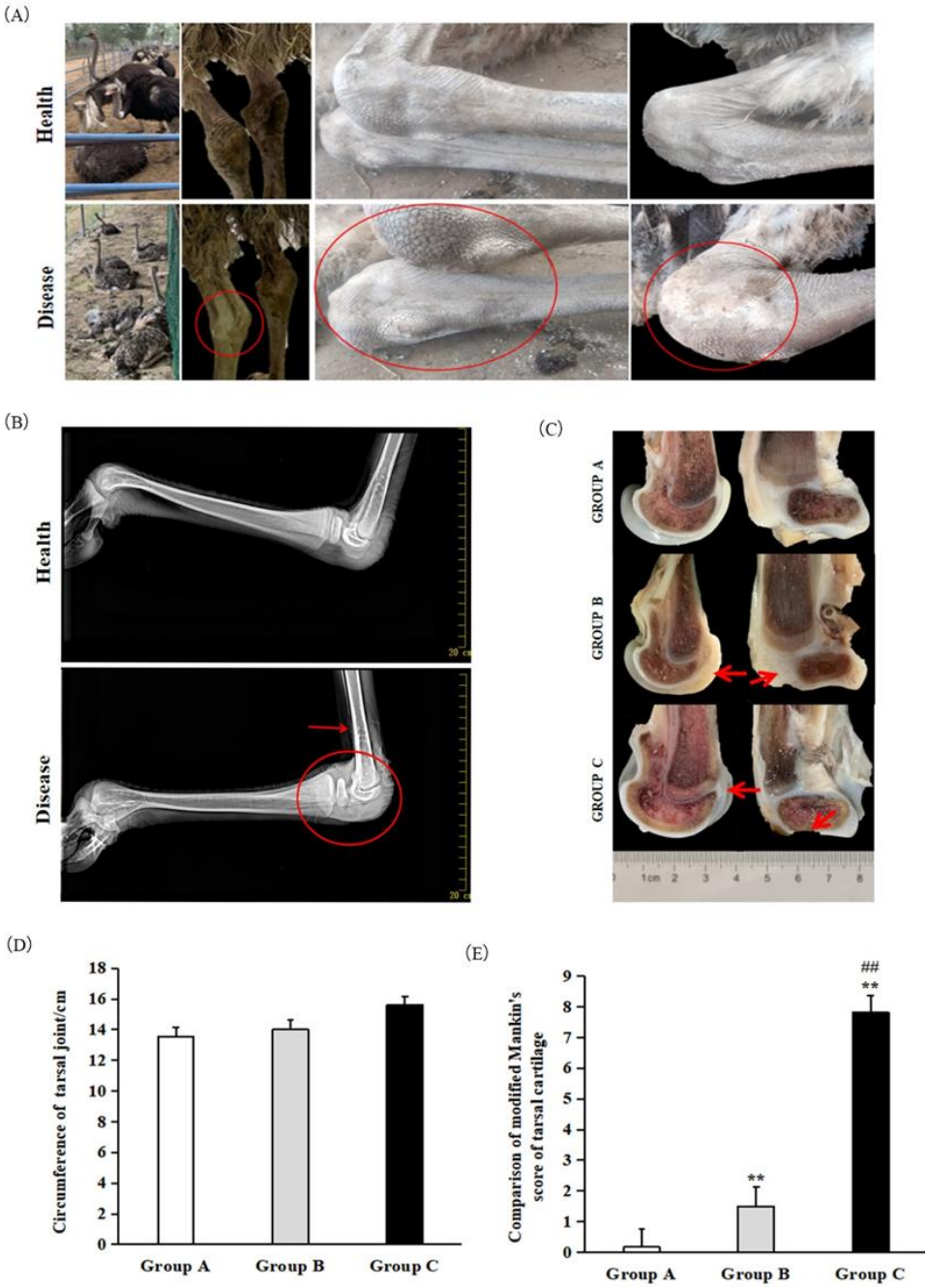

Fig. 1: General observation and identification of lesion degree in ostrich with toe leg disease. (A) The red circle shows that ostriches with sick toes and legs have tarsal joint swelling compared with healthy ostriches; (B) The arrows showed that compared with healthy ostriches, there were highlighted areas in the subchondral bone of tarsal joints of toe-leg diseased ostriches, suggesting osteosclerosis of the lower bone. Red circles indicate tarsal swelling, and small osteophytes on the convex side of the cartilage; (C) Anatomical comparison of ostrich tarsal joints in groups A, B and C, (D) Comparison of tarsal joint circumference in groups A, B and C, (E) Comparison of Mankin's scores for improved tarsal cartilage of healthy ostriches, the scores of groups B and C were very significant (P<0.01) greater than that of group A, and the scores of group C (P<0.01) were greater than that of group B. The data are presented as mean (M)±standard deviation (SD) (n = 6). Compared to group A, * indicates significant difference (P<0.05) and ** indicates that the difference is extremely significant (P<0.01). Compared to C and group B, # indicates significant difference (P<0.05), ## indicates that the difference is extremely significant (P<0.01)

groups B and C was significantly lower (P>0.05), while, the ratio of Bcl-2/Bax in group C was significantly lower than that in group B (P>0.05) (Fig. 4).

DISCUSSION

The results of our study revealed the distinct pathological alterations in ostriches afflicted with toe and leg disease, encompassing phenomena such as cartilage thickening, a diminished chondrocyte count, superficial staining of the cartilage matrix, incomplete tide marks, and reduced collagen levels. Additionally, there was a significant increase in chondrocyte apoptosis and altered expression of apoptotic proteins (Bcl-2 and Bax). Importantly, these changes demonstrated a correlation with the progression of disease duration, suggesting an exacerbation of chondrocyte apoptosis over time. This collective evidence supports the hypothesis that increased chondrocyte apoptosis serves as an underlying mechanism in the development of toe and leg disease in ostriches.

The experimental results of Cheng *et al.*, (2022) indicated that the OA model rats show drowsiness, decreased range of motion, knee swelling, rough and defective articular cartilage surface, with significantly reduced number of chondrocytes. Moreover, a significantly reduced staining area of safranin O staining was observed indicting the decline in the cartilage matrix in OA patients with severe decolorization of the damaged area. Besides, the Mankin's score of the OA group was found to be significantly higher than that of the healthy group, while the bone mass increased, and tissue became hardened. The observed pathological changes in our experiment align with the clinical findings in aforementioned study indicating a strong connection between the pathological changes and associated articular cartilage injury.

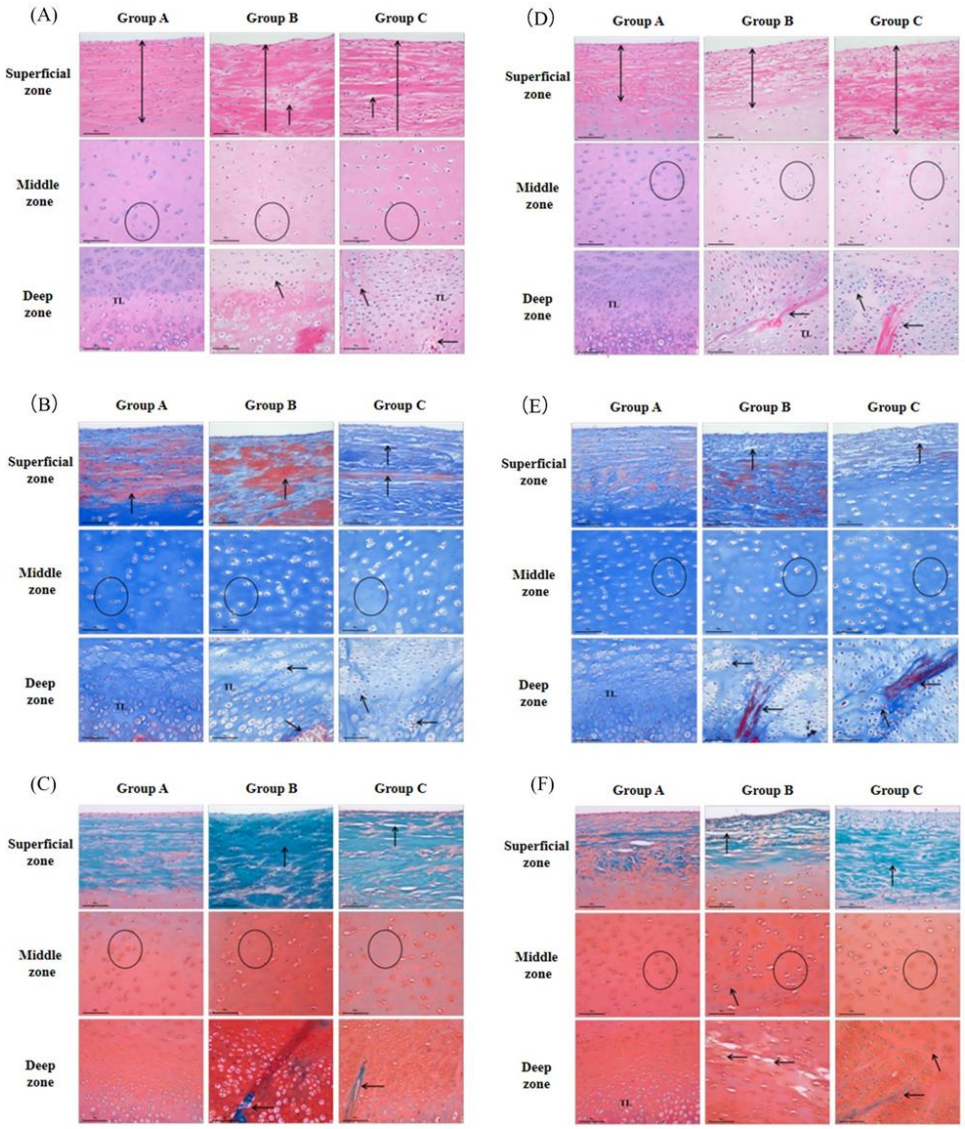

Fig. 2: Pathological changes in tarsal articular cartilage. (A) HE staining of the tarsal cartilage (concave) (B) Masson trichome staining concave of the tarsal cartilage (C) Results of tarsal cartilage concave face; Safranin O-solid green staining; (D) Tarsal cartilage convex HE staining result (E); Tarsal cartilage convex Masson staining result (F); Tarsal cartilage convex Safranin O-solid green staining result. In the HE staining results, the surface layer↑ showed thickening of the cartilage, and the deep↑ showed the vascular invasion tide line. TL is the tide line. The results of Masson staining showed that the cartilage matrix and collagen fibers were stained lightly, fibrosis was obvious, and collagen was significantly reduced. Safranin O-solid green staining showed that the proteoglycan staining in the cartilage matrix was lighter, the glycosaminoglycan content was reduced, and the fiber component increased. Magnification 400 ×, bar = 100 μm

Upon comparing the typical cartilage structure of humans (Wu *et al.*, 2016), rats (Rozi *et al.*, 2022), rabbits (Kim *et al.*, 2018) and ostriches, we observed fundamental similarities in superficial, transitional layer, tidal line, and calcification layer structures of articular cartilage across these species. The notable difference lies in the composition of the radiation layer encompassing the radiation cells and tide line. The radiation cells of human cartilage are large, irregular in morphology, multinucleated cells and the tide line is obvious; The radiation layer of mouse cartilage is typical mast cells without tide lines; the radiation layer of rabbit cartilage is a typical columnar cell layer and the cells are arranged in a columnar shape and perpendicular to the surface of the cartilage, and the tide line is obvious; while in ostrich cartilage, the radiation layer cells are small, multinucleated with irregular morphology and multicellular clustering, while the tide line are obvious. In summary, we can find that the tarsal cartilage structure of ostriches is similar to that of humans in structular compostion. Therefore, the study of ostrich leg and toe disease can refer to the pathological manifestations of human OA. However, OA is more prevalent in middle-aged and elderly people. Because of excessive weight-bearing or joint use, it promotes the occurrence of joint degenerative changes, thus causing the occurrence of OA. While on the other hand, the ostrich toe and leg disease primarily occurs in young ostriches aged 1-4 months. It has been reported that potential factors contributing to this phenomenon include issues like yolk sac malabsorption, excessive humidity during hatching, and low abdominal temperature during the hatching process (Tang *et al.*, 2012). However, it is important to note that the onset of diseases typically results from a combination of external environmental factors and internal elements. Under identical external environmental conditions, internal factors may serve as the primary cause of the disease. In present results, the main lesions of tarsal cartilage were the reduction of chondrocytes and the degradation of cartilage extracellular matrix. It is well known that chondrocytes are the only cellular component in articular cartilage. The extracellular matrix (ECM) of cartilage is the place where chondrocytes play physiological roles, and is the carrier for chondrocytes to absorb nutrients and transmit signals. Its metabolic balance maintains the normal function of cartilage tissue (Grogan *et al.*, 2014). Therefore, referring to the etiology of OA, we speculate that during the development of ostrich toe disease, the compensatory or feedback increase or decrease of certain cytokines may also change the biological environment of

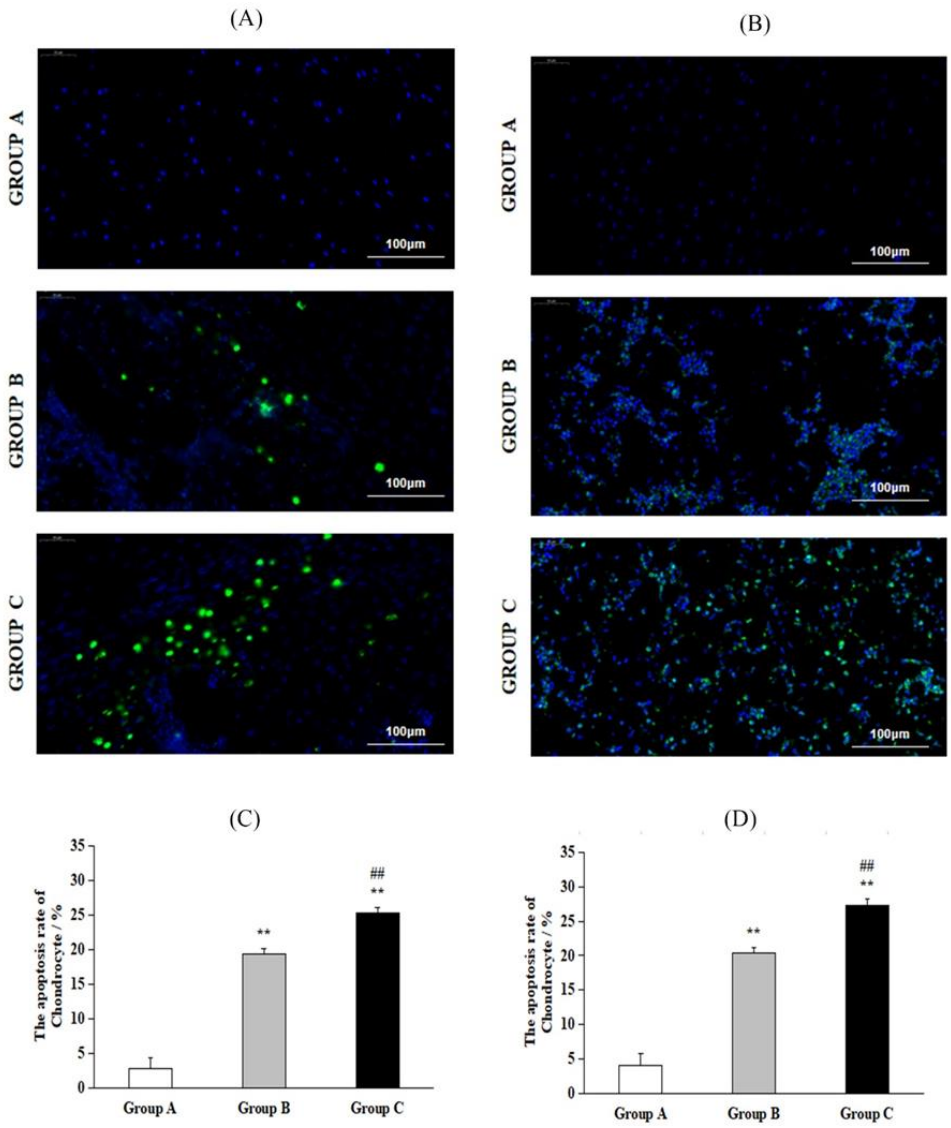

Fig. 3: Results of apoptosis in tarsal chondrocytes indicated by TUNEL Assays. (A) and (B) are TUNEL results of tarsal cartilage convex and cartilage concave, respectively, and the apoptotic cells were green and mainly located in the middle layer of cartilage (400×, bar = 100 μm); (C) and (D) are the apoptosis rate of chondrocytes of tarsal articular cartilage convex and cartilage concave respectively in tarsal joint. The chondrocyte apoptosis rates of tarsal cartilage convex and cartilage concave in groups B and C were significantly greater than those of group A (P<0.01), and group C was significantly greater than group B (P<0.01). The data is presented as a mean (M) ± standard deviation (SD) (n = 6). Compared to group A, * indicates significant difference (P<0.05) and ** indicates that the difference is extremely significant (P<0.01). Compared to C and group B, # indicates significant difference (P<0.05), ## indicates that the difference is extremely significant (P<0.01).

articular cartilage, result in abnormal apoptosis of chondrocytes which disrupts the metabolic homeostasis of the extracellular matrix, thereby disrupts the structural and functional integrity of articular cartilage. With the degradation of the ECM, its degradation products will further stimulate chondrocytes and synovial tissue to secrete IL-1β, stimulate the production of synovial fluid in the synovium, result in a compensatory increase in joint effusion, cause swelling of the tarsal joint (Rahmati *et al.*, 2017). Meanwhile, the integrity of the collagen network and the synthesis and storage of proteoglycans determine the physical properties of cartilage tissue (Bhosale, 2008). Once the metabolic balance is broken, the elastic components in the collagen network system are damaged, which resulted in a decrease in the hardness and elasticity of the cartilage. Due to the changes in the mechanical properties of the cartilage mentioned above, the long-term exercise of the ostrich with toe and leg disease is more likely to cause joint wear, resulted in the damage of cartilage tissue A certain degree of defect occurs. Moreover, there is a joint effect of pressure transmission and release between cartilage and subchondral bone. When the load is too large or the lasting mechanical stimulation exceeds the adaptation range of cartilage and subchondral bone, it will cause the local subchondral bone formation and regulate bone reconstruction, result in sclerosis of the subchondral bone (Loeser *et al.*, 2012).

Articular cartilage injury mediated by chondrocyte apoptosis is an important pathological feature of arthritis (Ma *et al.*, 2021), the reason for this is that apoptosis not only occurs in many normal tissues, Yet, while apoptosis is essential for preserving the stability of the internal environment, an inadequate or excessive occurrence of apoptosis can give rise to diseases. Even in healthy articular cartilage, chondrocyte apoptosis is present, albeit at a remarkably low rate of approximately 2-5%. Although, in cartilage 18-21% of chondrocytes showed apoptotic features in OA (Héraud *et al.*, 2000). The results of our experiment showed that the apoptosis rate of chondrocytes in the diseased group was significantly higher than that in the healthy group, which was consistent with the results of the aforementioned OA studies. Therefore, it can be inferred that the reduction of chondrocytes in the tarsal joint of ostrich toe leg disease may be caused by excessive apoptosis.

In the experiment of Zhang *et al.* (2019), the ratio of Bcl-2/BAX mRNA was sharply decreased in the model group for OA. Kourtis et al found that in the osteoarthritic samples, the mRNA expression levels of BAX genes were found significantly upregulated by signals which can

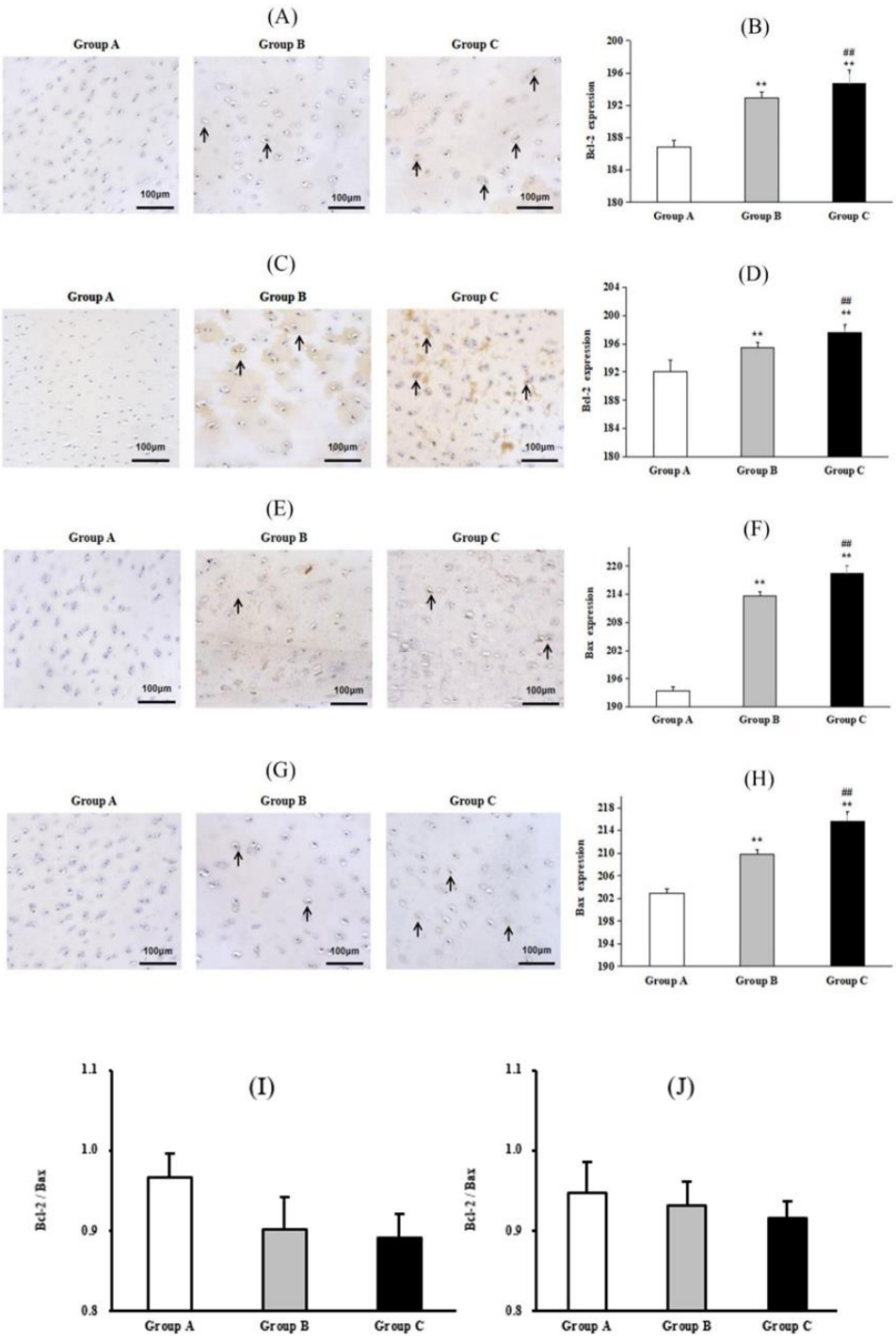

Fig. 4: Expression of Bcl-2 and Bax in cartilage convex and cartilage concave by IHC. (A) and (B) Expression of Bcl-2 in tarsal cartilage convex; (C) and (D) Expression of Bcl-2 in tarsal cartilage concave; (E) and (F) Expression of Bax in tarsal cartilage convex; (G) and (H) Expression of Bax in tarsal cartilage concave; where ↑ represents positive cells (400×, bar= 100 μm); (I) and (J) were the Bcl-2/Bax ratio results of tarsal cartilage convexity and cartilage concave, respectively. The data is presented as mean (M) ± standard deviation (SD) (n = 6). Compared to group A, * indicates significant difference (P<0.05) and ** indicates that the difference is extremely significant (P<0.01). Compared to group C and group B, # indicates significant difference (P<0.05), ## indicates that the difference is extremely significant (P<0.01).

activate apoptosis (Kourtis *et al.*, 2018). Iannone *et al.* (2005) found that Bcl-2 expression was increased in the site of severe cartilage damage in arthritis. Furthermore, in the investigation of the regulatory role of long noncoding RNA MEG3 in osteoarthritis through modulation of the miR-34a/Klotho axis, a substantial decrease in the expression level of Bcl-2 and a pronounced increase in Bax expression were noted in the osteoarticular mouse model group (Xiong *et al.*, 2022). Similarly, in the experiment conducted by Wan *et al.*, (2021), the ratio of Bcl-2/Bax was found to be significantly reduced in the mouse model group of OA. Bcl-2/Bax values were also found to be lower than those in the control group in the OA rat model group studied by Fan *et al.* (2018). The results of our experiment showed that the expression of Bcl-2 and Bax proteins was significantly increased and the ratio of Bcl-2/Bax significantly decreased in the tarsal joint cartilage of diseased ostriches, and results of the group C were more significant than those of group B. The above prompts that the Bcl-2 and Bax are involved in the apoptosis of chondrocytes in the tarsal joint of ostrich toe leg disease. In our experimental results, the expression level of Bcl-2 and Bax in tarsal cartilage have increased, however, the increase in Bax expression far exceeded than that of Bcl-2, so the Bcl-2/Bax ratio decreased, which promoted chondrocyte apoptosis, breaking the dynamic balance of extracellular matrix metabolism, ultimately destroying the structure. Such phenomenon affects the structure and function of articular cartilage, and eventually leads to the

occurrence of ostrich toe and leg disease. Therefore, this suggests that chondrocyte apoptosis may be the underlying mechanism of ostrich with toe-legged disease.

Conclusions: This study is an important landmark in regulating the underlying the potential pathogenic mechanism involved in ostrich toe-legged disease. The results indicated that in ostriches afflicted with toe-legged disease, a reduction in the number of chondrocytes within the tarsal cartilage was evident, coupled with matrix degradation. Notably, the severity of cartilage lesions exhibits a positive correlation with the extent of the overall lesion. The expressions of Bcl-2 and Bax proteins displayed a positive correlation with the degree of the lesion, indicating their involvement in the injury of the tarsal joint in toe and leg disease. Consequently, apoptosis and the apoptosis-related factors Bcl-2 and Bax are implicated in the pathogenesis of toe and leg disease in ostriches, shedding light on potential mechanisms underlying these pathological conditions.

Authors contribution: L Tang, M Xian, HX Zhou and BW Duan designed and carried out experiments, and M Xian, BW Duan collected samples and analyzed the data. BW Duan and M Xian wrote the manuscript, and all authors discussed the study. All authors approved the final version of this manuscript.

Conflict of interest: The authors declare no conflict of interest.

Acknowledgements: The authors are thankful to the Sanmu ostrich breeding farm in Mianyang city.

REFERENCES

Bhosale AM, Richardson JB, 2008. Articular cartilage: structure, injuries and review of management, Br Med Bull 87:77-95.

Cheng JH, Chou WY, Wang CJ, et al., 2022. Pathological, morphometric and correlation analysis of the modified mankin score, tidemark roughness and calcified cartilage thickness in rat knee osteoarthritis after extracorporeal shockwave therapy. Int J Med Sci 19:242-256.

Fan MP, Si M, Li BJ, et al., 2018. Cell therapy of a knee osteoarthritis rat model using precartilaginous stem cells. Eur Rev Med Pharmacol Sci 22: 2119-2125.

Go EJ, Kim SA, Cho ML, et al., 2022. A combination of surgical and chemical induction in a rabbit model for osteoarthritis of the knee. Tissue Eng Regen Med 19:1377-1388.

Grogan SP, Chen X, Sovani S, et al., 2014. Influence of cartilage extracellular matrix molecules on cell phenotype and neocartilage formation, Tissue Eng Part A 20:264-74.

Héraud F, Héraud A, Harmand MF, 2000. Apoptosis in normal and osteoarthritic human articular cartilage, Ann Rheum Dis 59:959-65.

Huang ZY, Wu RC, Ran JH, et al., 2018. A review of mitochondrial regulation of apoptosis. Jilin Med Sci 39: 1356-1357.

Iannone F, De Bari C, Scioscia C, *et al*., 2005. Increased Bcl-2/p53 ratio in human osteoarthritic cartilage: a possible role in regulation of chondrocyte metabolism, Ann Rheum Dis 64:217-21.

Kim JE, Song DH, Kim SH, *et al*., 2018. Development and characterization of various osteoarthritis models for tissue engineering, PLoS One 13:e0194288.

Kourtis A, Adamopoulos PG, Papalois A, *et al*., 2018. Quantitative analysis and study of the mRNA expression levels of apoptotic genes BCL2, BAX and BCL2L12 in the articular cartilage of an animal model of osteoarthritis, Ann Transl Med 6:243.

Loeser RF, Goldring SR, Scanzello CR, *et al*., 2012. Osteoarthritis: a disease of the joint as an organ, Arthritis Rheum 64:1697-707.

Li Y, 2021. Study on the effect and mechanism of DHA and EPA on the pathogenesis of osteoarthritis in rats. Northeast Agricultural University.

Mankin HJ, Dorfman H, Lippiello L, *et al*., 1971. Biochemical and metabolic abnormalities in articular cartilage from osteo-arthritic human hips. II. Correlation of morphology with biochemical and metabolic data. J Bone Joint Surg Am 53: 523-537.

Ma GG, Yang Y, Chen Y, *et al*., 2021. Blockade of TRPM7 alleviates chondrocyte apoptosis and articular cartilage damage in the adjuvant arthritis rat model through regulation of the indian hedgehog signaling pathway. Front Pharmacol 12: 655551.

Ma QY, Xu CY, 2021. Cat fracture treatment. Sichuan Animal & Veterinary Sciences 48:52-53.

Ni CH, Zeng SY, Chen Z, *et al*., 2021. Kruppel-like factor 4 upregulates the resistance to apoptosis induced by tumor necrosis factor α in synovial fibroblasts with rheumatoid arthritis. Eur J Inflamm 19: 1-7.

Peel MJ, Torres RSG, Ivančić M, *et al*., 2022. Management of intertarsal septic arthritis in an ostrich (Struthio camelus), Vet Med Sci 8:125-29.

Rahmati M, Nalesso G, Mobasheri A, *et al*., 2017. Aging and osteoarthritis: Central role of the extracellular matrix, Ageing Res Rev 40:20-30.

Rozi R, Zhou Y, Rong K, *et al*., 2022. miR-124-3p sabotages lncRNA MALAT1 stability to repress chondrocyte pyroptosis and relieve cartilage injury in osteoarthritis, J Orthop Surg Res 17:453.

Tang L, Zhang Y, Peng KM, 2012. Discussion on the causes and comprehensive prevention measures of toe and leg disease in young ostriches. Progress in Veterinary Medicine 5: 131-134.

Venäläinen E, Valaja J, Jalava T, *et al*., 2006. Effects of dietary metabolisable energy, calcium and phosphorus on bone mineralisation, leg weakness and performance of broiler chickens, British poultry science 47:301-10.

Wander KW, Schwarz PD, James SP, *et al*., 2000. Fracture healing after stabilization with intramedullary xenograft cortical bone pins: a study in pigeons, Vet Surg 29:237-44.

Wang SL, 2018. Prevention and treatment of chicken osteochondrosis. Livestock and poultry industry 29:116-118.

Willis S, Day CL, Hinds MG, *et al*., 2003. The Bcl-2-regulated apoptotic pathway, J Cell Sci 116:4053-6.

Wu Y, Cisewski SE, Wegner N, *et al*., 2016. Region and strain-dependent diffusivities of glucose and lactate in healthy human cartilage endplate, J Biomech 49:2756-2762.

Wan C, Tan HR, Yan J, *et al*., 2021. Internal heat acupuncture improves knee osteoarthritis injury in rats by regulating Bcl-2/Bax balance. J Basic Chinese Med 27: 432-435.

Xiong GX, Wang SL, Pan ZJ, et al., 2022. Long non-coding RNA MEG3 regulates the progress of osteoarthritis by regulating the miR-34a/Klotho axis. Ann Transl Med 10: 454

Yuan K, Wang D, Luan Q, et al., 2020. Whole genome characterization and genetic evolution analysis of a New Ostrich Parvovirus. Viruses 12:334.

Yuan CS, Guan YB, Li Z, 2022. Screening and verification of key genes for necrotizing apoptosis in osteoarthritis. Chinese J Tissue Engin Res 27: 695-700.

Zhang J, Li Q, Chang S, 2019. The effects of particle density in moxa smoke on the ultrastructure of knee cartilage and expressions of TNF-α, IL-1b, BAX, and Bcl-2 mRNA in a rat model for osteoarthritis. J Cell Biochem 120:6589-6595.